

Disturbance due to Measurements on a Chaotic System

Manish Ram Chander*

Institute of Mathematical Sciences, Taramani, Chennai 600113, India

Arul Lakshminarayan†

Department of Physics, Indian Institute of Technology Madras, Chennai 600036, India

Abstract

We study the quantized kicked top's dynamics under projective measurements especially with an aim to connect macroscopic realism (macrorealism) and chaos. The kicked top is a classically chaotic system, and macrorealism is a set of assumptions regarding how systems should behave according to classical intuition which is at present being tested in experiments. Using the no-signalling in time condition, a derivative of macrorealism, we define measures of disturbance due to measurements in order to study the effects of chaos. Restricting to cases which allow a meaningful study of this question, our results strongly suggest that chaos is unfriendly to macrorealism.

* manishd@imsc.res.in

† arul@physics.iitm.ac.in

I. INTRODUCTION

We aim to connect classical chaos and macrorealism, a set of assumptions proposed to test the limits of quantum mechanics. They codify the intuition of how macroscopic objects behave [1, 2] and are in direct contradiction to postulates of quantum mechanics when applied to macroscopic systems. These assumptions allow derivation of the Leggett-Garg inequalities and the no-signalling in time (NSIT) condition [3], each of which must be respected by physical systems obeying the pertinent assumptions. Here we employ the NSIT condition (simpler of the two) to answer whether quantized chaotic systems could be especially violative against the tests. The subject of macrorealism has been extensively studied lately in various directions; see [4] for a review, and [5–7] for interesting recent developments.

Quoting [2], macrorealism states that (1) “a macroscopic system with two or more macroscopically distinct states available to it will at all times be in one or the other of these states.” (2) “It is possible in principle to determine which of these states the system is in without any effect on the state itself or on the subsequent system dynamics.” (3) “The properties of ensembles are determined exclusively by initial conditions (and in particular not by final conditions)”. The NSIT condition follows from these assumptions, as shown in [3]. The idea of macroscopic distinctness is not uniquely defined and is reviewed in [8].

In this study we consider the disturbance due to projective measurements made by Alice on those made by Bob; two canonical observers studying the well-studied kicked top [9–15], a generic Hamiltonian system with an integrable to chaotic transition. Quantifying the disturbance in the spirit of NSIT condition, we shall make the said connection between chaos and macrorealism. The Hamiltonian is

$$H(t) = J_y \frac{\pi}{2} + \frac{\kappa_0}{2j} J_z^2 \sum_{n=-\infty}^{\infty} \delta(t - n) \quad (1)$$

where κ_0 is a parameter signifying the kick strength. The top displays chaos in the classical limit as κ_0 increases beyond 2 and becomes almost fully chaotic for $\kappa_0 > 6$. The corresponding quantum unitary map is the Floquet operator connecting states across a time-period (here chosen as unity) is given by

$$U = \exp(-i\kappa_0 J_z^2/2j) \exp(-iJ_y \pi/2) \quad (2)$$

which we shall often write as $U = TR$ where $T = e^{-i\kappa_0 J_z^2/2j}$ comes from the twist and $R = e^{-iJ_y\pi/2}$ comes from the rotation. This system becomes increasingly macroscopic with increasing j , and therefore is relevant for the study of macrorealism tests.

Quantum mechanics intrinsically violates the assumptions of macrorealism. Therefore it is not a surprise that calculations would lead to violations of NSIT, especially for small j . To answer whether the degree of discord between the two depends on chaos or not, it is imperative to focus on identifying direct effects of chaos and filter out intrinsic violations arising from other known sources, such as incompatible measurements. Restricting to special initial states and measurement schemes will enable us to do so.

A. NSIT and two measures

We want to study how much Alice's measurement can affect Bob's measurement. The question of how much disturbance is there however, immediately begs another question - when were the measurements made? Therefore, the study must necessarily get entangled with discussions of temporal separation between the measurements.

Suppose that Alice and Bob measure observables $\mathbf{J} \cdot \hat{\mathbf{a}}$ and $\mathbf{J} \cdot \hat{\mathbf{b}}$ respectively, on a kicked top possessing total angular momentum j . Let t_0 be the initial time, and let Alice make her measurement at time t_α and Bob make his at t_β , with $t_0 < t_\alpha < t_\beta$.



Figure 1: The measurement timeline. Time increases along the axis towards right.

According to macrorealism, “a measurement does not change the outcome statistics of a later measurement”. This is the no-signalling in time statement [3]. Its violation immediately implies that Bob's unconditional (when Alice does not measure) and conditional probability (when Alice measures) distributions are different.

Let $P(b, a; t_\beta, t_\alpha)$ be the joint probability distribution for Alice's and Bob's measurements described above. Here b is Bob's outcome and a is Alice's; t_β, t_α serve as parameters of the distribution, highlighting respective measurement times. Further, we define $P_B(b; t_\beta)$ as the unconditional probability for Bob's measurement of eigenvalue b at t_β and $P_C(b; t_\beta, t_\alpha)$ as

the conditional probability for the same. It follows from the definition that

$$P_C(b; t_\beta, t_\alpha) = \sum_a P(b, a; t_\beta, t_\alpha), \quad (3)$$

and NSIT condition when cast into an equation, becomes

$$\forall t_\alpha < t_\beta : P_B(b; t_\beta) = P_C(b; t_\beta, t_\alpha) \quad (\text{true under MR}). \quad (4)$$

Alice makes only one measurement before Bob, and when Bob eventually compares the probability distributions he gets with and without the measurement, the results may be different. We consider two measures to quantify this difference:

First is the Hellinger distance [16]. If we take N ordered pairs of events (x_i, y_i) with p_i (q_i) being the probability corresponding to x_i (y_i), then, the Hellinger distance between the distributions is defined as

$$H(p, q) = \frac{1}{\sqrt{2}} \sqrt{\sum_{k=1}^N (\sqrt{p_i} - \sqrt{q_i})^2} \quad (5)$$

The distance is bounded between 0 and 1. Note that if and only if $p_i = q_i$ for each i , this distance is zero, and becomes maximum whenever $p_i = 1, q_j = 1; i \neq j$. This observation reveals that $H(P_B, P_C)$ is suitable for implementing NSIT conditions.

Another simple measure is the difference in the number of accessible states Bob has in his measurement: difference in how many values of $\mathbf{J} \cdot \hat{\mathbf{b}}$ could he have got in the two cases. This measure can be defined using the participation ratio. Suppose that P is a probability mass function for X which can take values $\{x_1, x_2, \dots, x_n\}$. Then

$$W(P) = \frac{1}{\sum_k P(x_k)^2} \quad (6)$$

is a good measure of how much the distribution P is spread, being bounded between 1 and n . We can compute it for P_B and P_C to get the accessible states. Then we can define

$$\Delta(t_\beta, t_\alpha, j, \kappa_0) = \frac{1}{\sum_b P_C(b; t_\beta, t_\alpha, j, \kappa_0)^2} - \frac{1}{\sum_b P_B(b; t_\beta, j, \kappa_0)^2} \quad (7)$$

as the measure of disturbance, which is bounded between $2j$ and $-2j$. As Δ increases, we see intuitively that measurement gets less and less “classical”.

Regarding the temporal separation $t_\beta - t_\alpha$, in general Bob may choose to vary his measurement time from $t_\beta = 0$ to ∞ , according to an arbitrary probability distribution. Then,

for a fixed t_β , Alice may choose to measure at any time before Bob, according to a probability distribution of her choice. Simplest examples would be the delta and the uniform distributions for both of them. We restrict the study to the following scenario:

- Alice measures at a fixed time interval before Bob (the delta distribution), and Bob's time is a uniform random variable in a range $(1, T)$.

This set up shall capture several features of interest.

II. MEASUREMENTS AND RESULTS

A. Alice's measurement

Here we zoom in on what Alice's measurement does to the system, and discuss restrictions on $\hat{\mathbf{a}}, \hat{\mathbf{b}}$, the axes of measurements. Firstly, note that in calculating (3), Alice's action can be considered as a measurement that reduces the original pure state to a mixed state. To see this, let ρ_α be the state before measurement and suppose that the projectors of $\mathbf{J} \cdot \hat{\mathbf{a}}$ are labeled by $\{A_m\}$. Then

$$\rho'_\alpha = \sum_m A_m \rho_\alpha A_m \quad (8)$$

is the claimed mixed state post measurement. Subsequently, evolution occurs for $t_\beta - t_\alpha$, after which Bob measures and finds the distribution P_C :

$$P_C(b; t_\beta, t_\alpha) = \text{Tr}[U_{\beta\alpha} \rho'_\alpha U_{\alpha\beta} B_b] = \sum_m \text{Tr}[U_{\beta\alpha} A_m \rho_\alpha A_m U_{\alpha\beta} B_b]. \quad (9)$$

We use $U_{\beta\alpha}$ for the evolution operator from t_α to t_β . Multiply and divide by $\text{Tr}[\rho_\alpha A_m]$ for each term in the sum, to get

$$\sum_m \text{Tr}[U_{\beta\alpha} \rho_m U_{\alpha\beta} B_b] \text{Tr}[\rho_\alpha A_m]$$

where $\rho_m = A_m \rho_\alpha A_m / \text{Tr}[\rho_\alpha A_m]$. This is of course $\sum_m P(b, m; t_\beta, t_\alpha)$. This result is same as (3) and therefore the claim is established.

Next, note that measurements involving non-commuting operators will give violations that typically would get recorded by our distances, but would have absolutely nothing to do with chaos. Avoiding them would decrease noise, and hence allow a better understanding

of the effects that do arise from chaos. Therefore, we restrict to $\hat{\mathbf{a}} = \hat{\mathbf{b}}$ case, and henceforth work with density matrices in the $\mathbf{J} \cdot \hat{\mathbf{a}}$ eigenbasis $\{|\hat{\mathbf{a}}, m\rangle\}$.

The origin of violations for such cases lies in the removal of off-diagonal terms from the density matrix, because of Alice's measurement. To see this, suppose $\rho_\alpha = \sum_{m,n} \varrho_\alpha^{mn} |\hat{\mathbf{a}}, m\rangle\langle\hat{\mathbf{a}}, n|$ is the expansion of the state before Alice's measurement and let $A_k = |\hat{\mathbf{a}}, k\rangle\langle\hat{\mathbf{a}}, k|$. Then post measurement,

$$\begin{aligned} \rho'_\alpha &= \sum_k A_k \rho_\alpha A_k = \sum_{m,n,k} \varrho_\alpha^{nm} \delta_{km} \delta_{nk} |\hat{\mathbf{a}}, k\rangle\langle\hat{\mathbf{a}}, k| \\ &= \sum_k \varrho_\alpha^{kk} A_k \end{aligned} \quad (10)$$

Note that the diagonal terms are unchanged. Therefore, deletion of off-diagonals leads to all the observed differences between P_B and P_C . As time evolves, these non-diagonal entries effect the probabilities of measurement, because states evolves via conjugation by U . Motivated by this, we consider the l_1 norm of coherence [17]

$$C_A(t_\alpha^-) = \sum_{k \neq m} |\varrho_\alpha^{km}| \quad (11)$$

as a measure of disturbing power, because it measures strength of the off-diagonals in the matrix at time t_α^- , just before Alice's measurement. Here A in the subscript denotes the basis chosen by her. When it is zero, Alice causes no disturbance, and when it is large, intuitively, her measurement becomes more destructive. As κ_0 increases, C_A accentuates for initially localized states because of the non-trivial action of twist operator T (discussed in appendix). This leads to increased violation due to Alice's measurement, which is seen in the results below.

B. Fixed kick difference between measurements

Alice and Bob decide on $t_\beta - t_\alpha = n$, where Bob's time of measurement t_β is a uniform random variable over the set $\{n, n+1, \dots, n+T\}$. As a result, any distance computed between P_B and P_C which depends on t_β is another random variable. For a distance function $d(t_\beta, t_\alpha)$, we define $d_n(t_\beta) \equiv d(t_\beta, t_\beta - n)$, whose average is given by [18]:

$$\langle d_n \rangle = \frac{1}{T+1} \sum_{j=0}^T d_n(n+j). \quad (12)$$

Here d may be H or Δ . In the following, we look at this average as a function of κ_0 for two special coherent states of the kicked top: $|\hat{\mathbf{y}}, j\rangle$, which corresponds to a fixed point in classical map, and $|\hat{\mathbf{z}}, j\rangle$, which is part of a period-4 cycle classically. Being coherent [19, 20], they come closest to points in the phase space, which are classical states. Further, they both display quantum signatures of chaos [15] when corresponding classical orbits lose stability with increase in κ_0 . Therefore, they are good examples for studying effects of chaos in Δ and H . We push their further discussion to the appendix for clarity. At first, we set $\hat{\mathbf{a}} = \hat{\mathbf{b}} = \hat{\mathbf{z}}$, later discussing the generalization.

Even-odd n differences in J_z measurements

If Alice and Bob both measure J_z , the violations recorded in Δ and H are critically dependent on whether n is even or odd, for both the initial states. At $\kappa_0 = 0$, we see that for odd n , Δ and H are non-zero (figure 2), whereas for even n , both are zero.

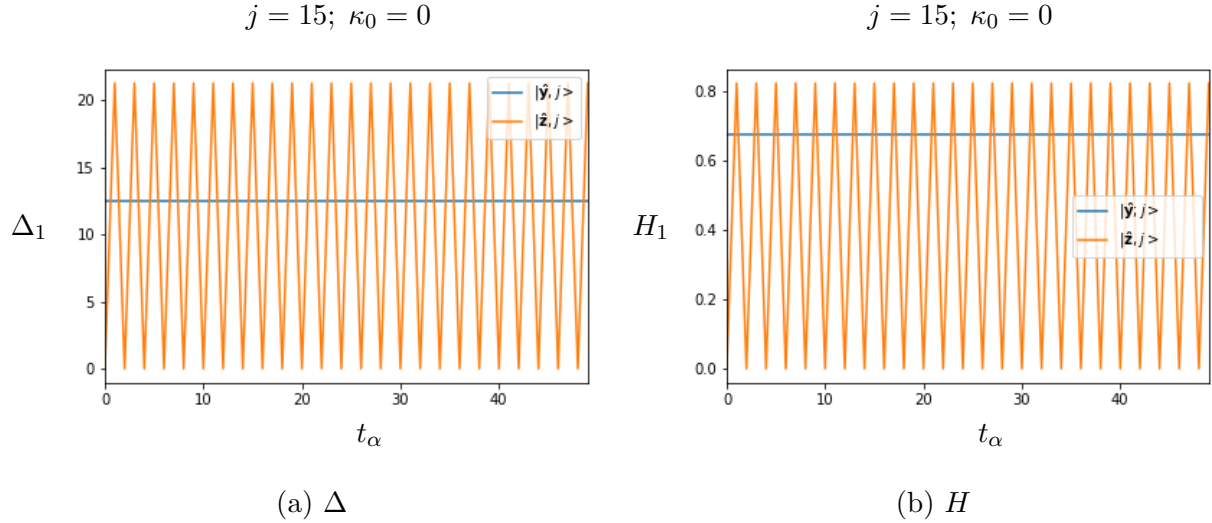


Figure 2: H_1, Δ_1 disturbance at $\kappa_0 = 0$. This plot is for $n = 1$, but applies to all odd n values. These

This happens because of the specific initial states and measurement axis. When undisturbed, the state $|\hat{\mathbf{z}}, j\rangle$ evolves to give the cycle

$$|\hat{\mathbf{z}}, j\rangle \rightarrow |\hat{\mathbf{x}}, j\rangle \rightarrow |\hat{\mathbf{z}}, -j\rangle \rightarrow |\hat{\mathbf{x}}, -j\rangle \quad (\text{repeat}). \quad (13)$$

At even t_α , state returns to a J_z eigenstate and hence Alice's measurement creates no effect.

These cases correspond to zero values seen in figure 2. At odd t_α however, she produces mixture of J_z eigenstates, which is invariant under R^2 . If then Bob measures at even t_β , so that n is odd, what would have been a J_z eigenstate for him without the measurement, becomes a mixture too. These cases correspond to the maxima seen in figure 2. For even n and odd t_α , using the fact that measurement axis is common and that mixtures produced are symmetric under R^2 , it follows that $\Delta, H = 0$.

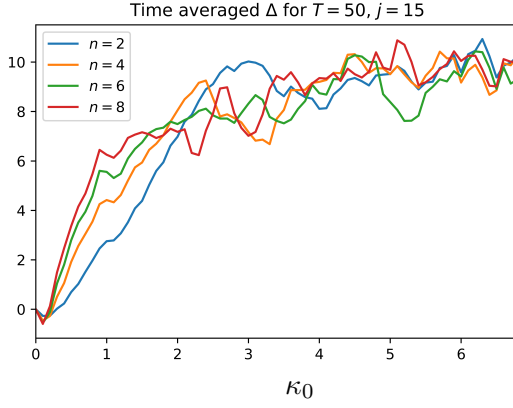
For initial state $|\hat{\mathbf{y}}, j\rangle$, there is no evolution for $\kappa_0 = 0$. Thus, Alice's measurement can only reduce it to one mixed state which is again invariant under R^2 , but changes under R . Again, as a result, odd n give violation, whereas even n do not. This time however, there are no oscillations as t_β varies.

So in plain rotation itself (when there is no chaos), we see significant violation of NSIT corresponding to odd values of n . This effect, by continuity persists even when κ_0 increases, and for the purposes of establishing a connection between chaos and the signalling, it is unwanted. Therefore, we turn out attention to only even n for both the states.

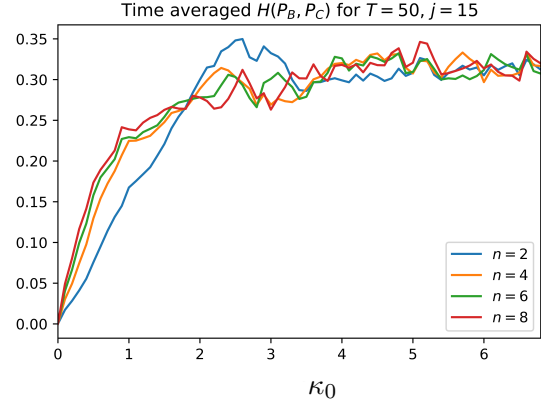
C. Results for $|\hat{\mathbf{z}}, j\rangle$ and $|\hat{\mathbf{y}}, j\rangle$

Figure 3 shows results for both Δ and H for $|\hat{\mathbf{z}}, j\rangle$. The qualitative picture seen in both is similar. The numbers are on different scales, but tend to saturate in the range $\kappa_0 = 3$ to 4, beyond which the differences in different n are lost. Physically, it means that if there is strong mixing, on average it doesn't matter how long ago Alice measured on the system. Her measurement causes an equally powerful effect, provided, she measures even periods before Bob. The disturbance leads to an enlargement in Bob's outcome possibilities, on an average. This in fact is seen in all results. The 4-period cycle corresponding to this state undergoes a change of stability at $\kappa_0 = \pi$. We identify the saturation-like behavior as an effect of this and the subsequent bifurcations with increase in κ_0 .

Figure 4 shows comparison of Δ with the coherence measure C_Z for this state. The 4-period cycle associated with it is stable whenever $(2 \cos \kappa_0 + \kappa_0 \sin \kappa_0)^2 < 4$. As a result, in the interval $[0, 7]$ there are 4 points where the stability of cycle changes. These are $\kappa_0 = 0, \pi, \sim 5.6$ and 2π . Till $\kappa_0 = 1$, the cycle remains close to stable-unstable boundary, becoming stable afterwards. This stability is marked with a slower spread of initially localized density out of the equator belt, which corresponds with the fall in $C_Z(\rho)$ beyond 1. At π it again becomes



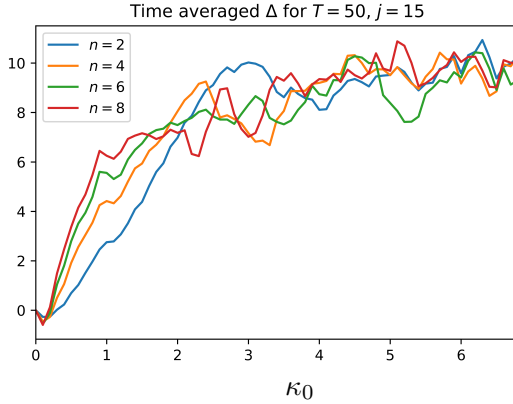
(a) Δ , time averaged



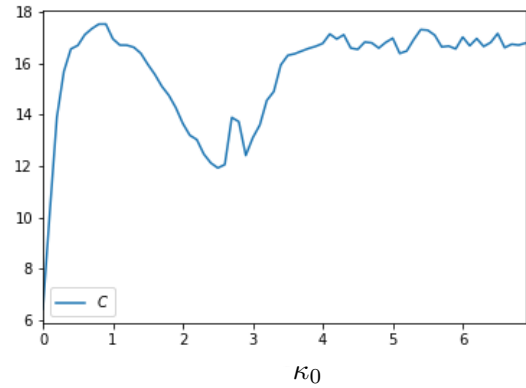
(b) H , time averaged

Figure 3: Plot for Δ and H . Measuring J_z for initial state $Z_j, j = 15$. Each of the cases $n = 2, 4, 6, 8$ has been obtained via time averaging with $T = 50$. The shape of the curves is essentially unchanged for larger T . Notice that saturation starts between 3 and 4, beyond which difference in n is lost.

unstable, which makes the coherence increase. Beyond 4, chaos becomes quite prominent over the whole sphere, and the windows of stability become smaller.



(a) Δ , time averaged



(b) C_Z , time averaged

Figure 4: Comparing the distance function and the coherence measure. Both display a characteristic signature of chaos at $\kappa_0 \sim \pi$. The plateau shows that in the chaotic limit, the number of off-diagonals saturate, and the violation is maximized. The behaviour before $\kappa_0 = \pi$ in (b) is also explained by the stability analysis of the cycle; from $\kappa_0 = 0$ to $\kappa_0 = 1$, the cycle is very close to the stable-unstable boundary, after which it becomes stable.

Figure 5 shows the contour plots corresponding to the time averaged plots in 4. Note that in (a) the oscillatory behaviour in Δ is lost for $\kappa_0 > \pi$. Similar effect is seen in (b), where oscillations become less prominent beyond this point. Both the results highlight that system tends to forget the sharp distinction between even t_α and odd t_α because of chaos, which exists from $\kappa_0 \sim 1$ to 3.

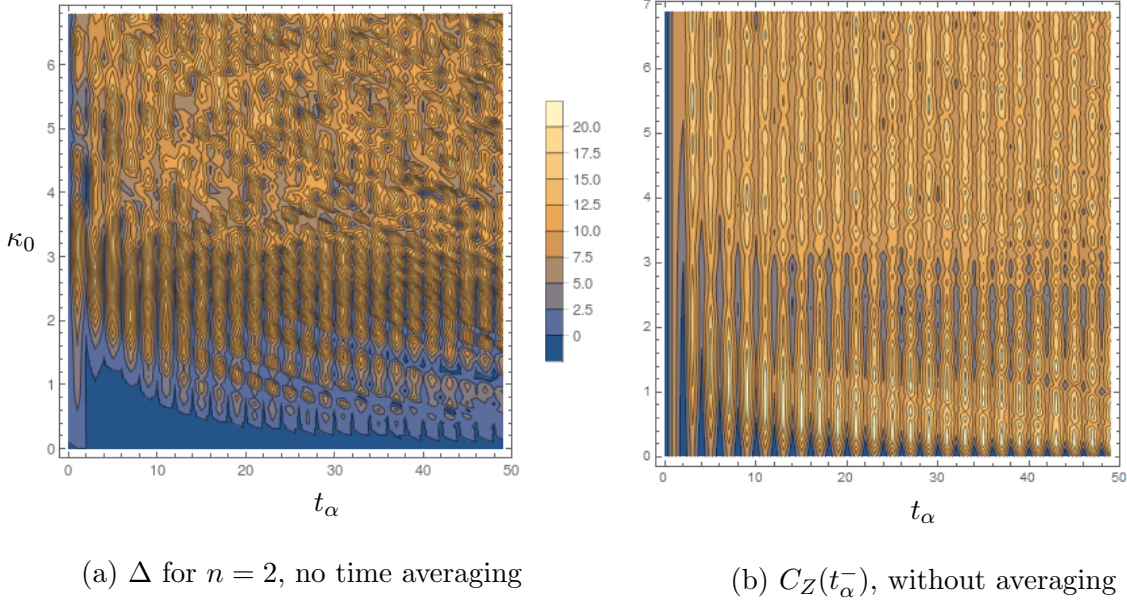
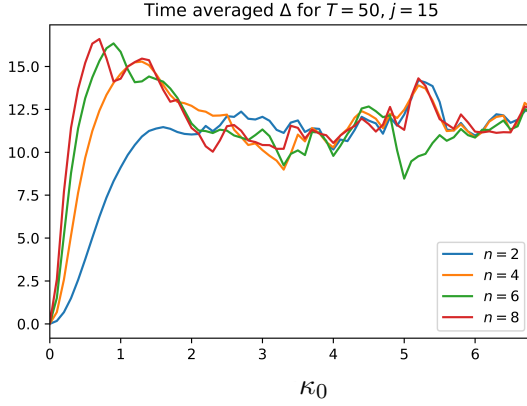


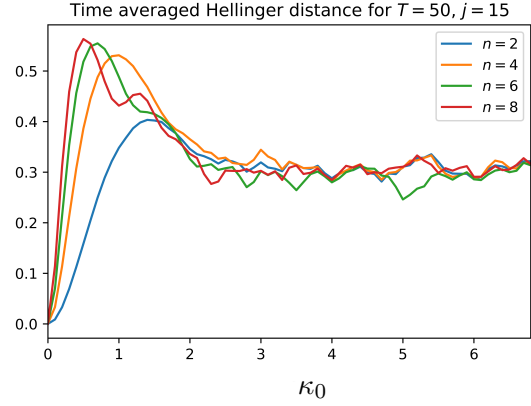
Figure 5: Contour plots for the averages in figure 4. Note the change in behaviour of oscillations beyond $\kappa_0 \sim \pi$. In between $\kappa_0 = 1$ and 3, the measurements at odd t_α create disturbance in Δ, H , but those made at even t_α are still reticent because the state $\rho(t_\alpha^-)$ is close to J_z eigenstate.

Figure 6, 7, 8 show the results for $|\hat{\mathbf{y}}, j\rangle$ state. A clear repetition of the earlier patterns is seen, however the point where functions saturate is $\kappa_0 = 2$, where the classical fixed point loses its stability.

These results strongly suggest an increase in κ_0 leads to more prominent violations and coherence, which we interpret as the disturbance power. It is important to emphasize that the results hold for general case. The apparent contradictions in odd n cases, for example, are distractors; see figure 9. The differences seen arise because of the special nature of the states and the axis of measurement. Everything is basically a rotation effect, as explained in the earlier section. However, it is interesting to note that in $|\hat{\mathbf{z}}, j\rangle$ state the system has not forgotten this rotation even when κ_0 is very large.

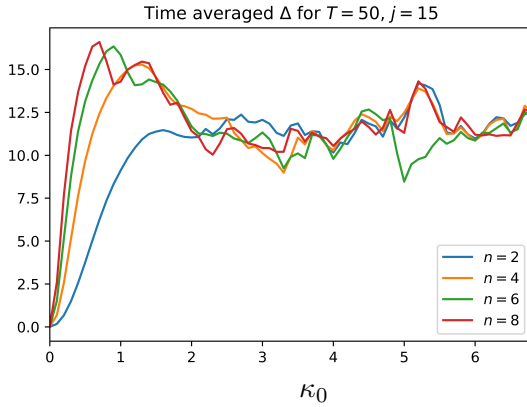


(a) Δ , time averaged

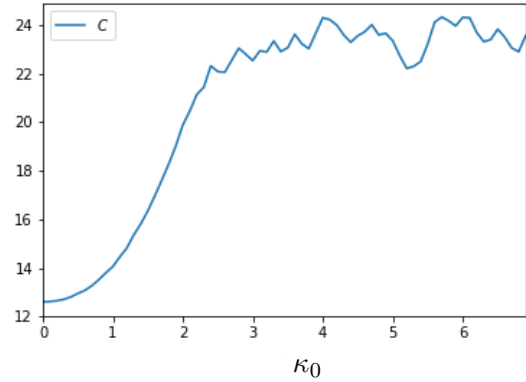


(b) H , time averaged

Figure 6: Plot for H and Δ for $|\hat{\mathbf{y}}, j\rangle$ state. Several features are as they were in the case of $|\hat{\mathbf{z}}, j\rangle$. Note however, that the peaks occur around 2 where the FP loses its stability. For small κ_0 , the prominent difference for different n values arises because of time evolution for the state localized in the regular region.



(a) Δ , time averaged



(b) C_Z , time averaged

Figure 7: Comparing Δ with $C_Z(\rho)$, for $|\hat{\mathbf{y}}, j\rangle$. The large value of coherence at $\kappa_0 = 0$ is due to J_z coherence basis for a J_y eigenstate.

The measurements could also be taken along other axes, (still keeping $\hat{\mathbf{a}} = \hat{\mathbf{b}}$) but would lead to similar conclusions. That's because in the large j limit the pertinent states would be dominated by a select few eigenstates in $\mathbf{J} \cdot \hat{\mathbf{a}}$ basis. As κ_0 would increase, additional terms appear in the density matrix (see appendix) for Alice's basis, leading to an increase in coherence and thereby an increase in Δ and H . We expect that even-odd effect for these

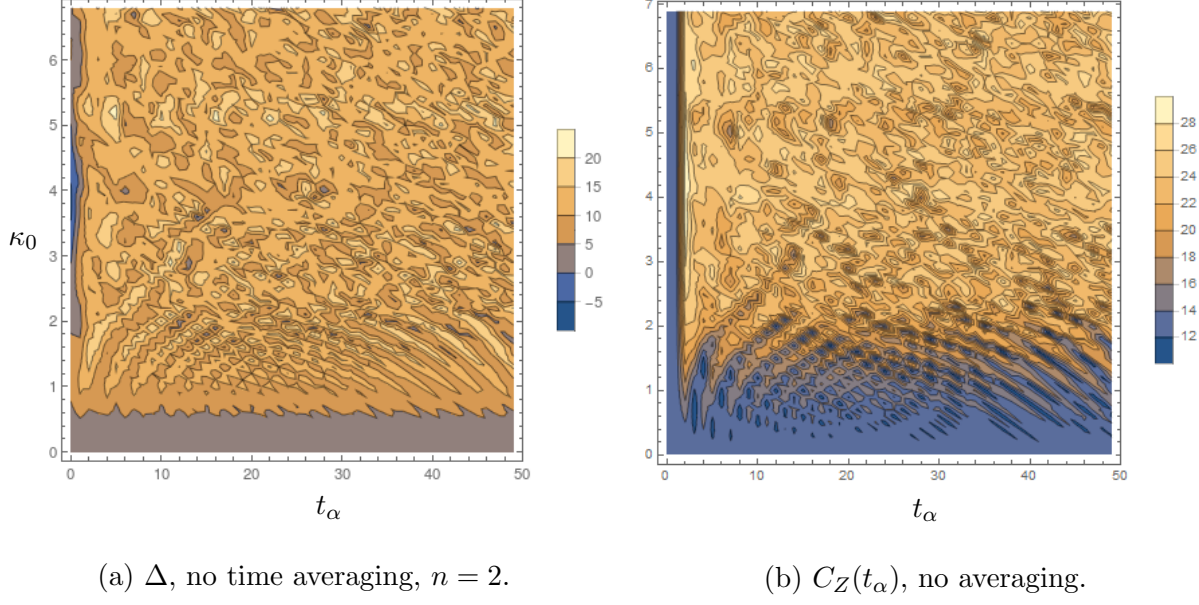


Figure 8: Contour plots for the averages in figure 7. The distance Δ and coherence C_Z are in direct correspondence here. At $\kappa_0 = 2$, the fixed point becomes unstable, which corresponds to a sharp increase in both.

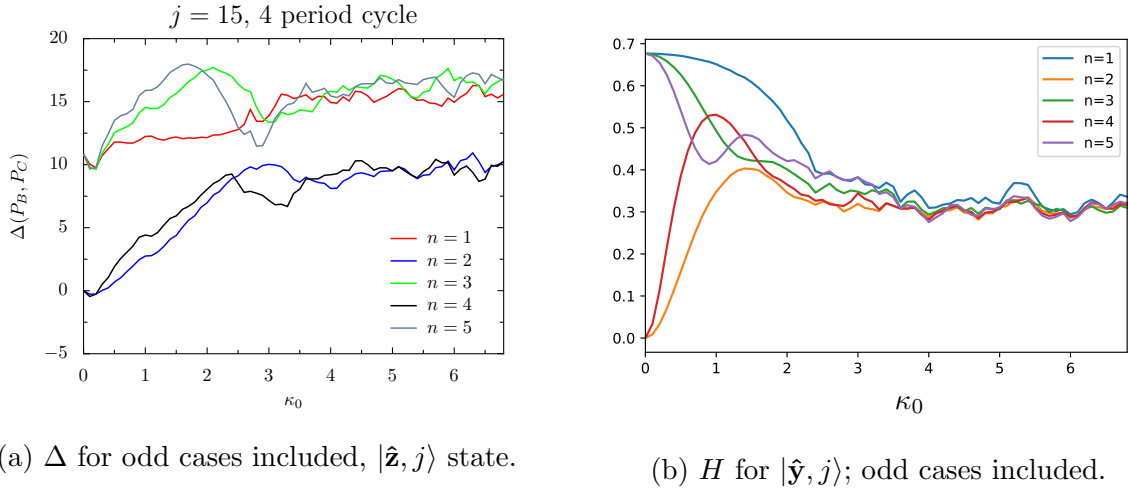


Figure 9: Some odd n cases. For low κ_0 values, pure rotation effects produce the difference, which for the $|\hat{\mathbf{y}}, j\rangle$ do vanish in the chaotic limit, whereas for $|\hat{\mathbf{z}}, j\rangle$, they persist.

cases will modify suitably.

We note that this result is linked soundly with the intuition of chaotic systems. In the classical case, a density localized in any region where the Lyapunov exponent is positive, stretches exponentially with time. As a result it is more likely to spread over a compact

phase space faster than a density localized in any regular region. In quantum case, the analogue of such a density is the Husimi distribution, a close associate of Wigner function, which is extensively used in field of quantum chaos[21, 22]. It displays similar effects, if one starts from a coherent state. Due to mixing of orthogonal eigenstates due to quantum dynamics, largely delocalized states get produced with time. This delocalization is in direct contradiction with the first assumption of macrorealism, because it allows a faster and more prominent superposition between macroscopically distinct quantum states.

III. SUMMARY AND CONCLUSION

We addressed the question of connection between chaos and macrorealism, by employing the no-signalling in time condition. Using it, we constructed two measures for disturbance produced by Alice’s measurement. Restricting to the relevant cases, we showed that onset of chaos and instability leads to larger disturbance, and disturbing power. We also showed that long-time average of disturbances is largely independent of the exact difference $t_\beta - t_\alpha$ in the chaotic limit. The dynamics can lead to formation of different equivalent sets of n values, within which these differences almost completely vanish. All this was done using two independent measures. We also found that l_1 norm of coherence is a good operational measure of disturbance power in the study.

The restrictions were on the initial states, the observables chosen, and then on the timing scheme. Chosen states display signatures of chaos, and hence they are appropriate for the question. Different axes of measurement lead to identified non-commutative effects, which were to be avoided. Regarding restriction to J_z measurements, we argued that the common measurement axis could have been chosen arbitrarily, and the results would not have changed. Lastly, our timing scheme allowed us to show that even though chaos tends to reduce the dependence of disturbance on $t_\beta - t_\alpha$, the details clearly shows that it might not be able to remove it completely.

We also highlighted how these results are in tune with the intuition of chaotic systems. The evidences considered show that chaos highlights the “non-classical” features of quantum mechanics. Therefore, experimental tests of macrorealism on chaotic systems may be particularly useful to study the universality of quantum mechanics.

APPENDIX: CLASSICAL AND QUANTUM DYNAMICS

Here we review the classical limit, focusing on the chosen initial states, followed by study of their quantum evolution. The latter explains how an increase in κ_0 leads to an increase in $C_A(\rho)$ for localized states.

A. Classical Map

Taking the limit of $j \rightarrow \infty$ in (1) with $J = \sqrt{j(j+1)}$ gives us the classical Hamiltonian. If we think of the classical vector \mathbf{J} in spherical polar coordinates, so that

$$\mathbf{J}/J = (\sin \theta \cos \phi, \sin \theta \sin \phi, \cos \theta), \quad (14)$$

solving the Hamilton's equations (taking $q = \phi$, $p = \cos \theta$) it is easily seen that the δ kick is an impulsive rotation of \mathbf{J} about z axis by an angle $J_z \kappa_0$, where $J_z = J \cos \theta$. During the kick, the rotation bit of Hamiltonian is negligible and thus Hamilton's equation integrates to give

$$\phi(n^+) - \phi(n^-) = \int_{n^-}^{n^+} dt \dot{\phi} = \int_{n^-}^{n^+} dt \frac{\partial H}{\partial p} = J \kappa_0 \cos \theta \int_{n^-}^{n^+} dt \sum_{-\infty}^{\infty} \delta(t - k) = J_z \kappa_0 \quad (15)$$

for any n . Therefore, we see that this system is rotating about two axes in each turn; by a constant angle of $\frac{\pi}{2}$ around the y axis, and by a variable angle around the z -axis. This "variation" in the angle is a necessary ingredient of chaos.

This system evolves according to a 2D map - because \mathbf{J}^2 is a constant of the motion - which is

$$X_i = Z_{i-1} \cos(\kappa_0 X_{i-1}) + Y_{i-1} \sin(\kappa_0 X_{i-1}) \quad (16)$$

$$Y_i = -Z_{i-1} \sin(\kappa_0 X_{i-1}) + Y_{i-1} \cos(\kappa_0 X_{i-1}) \quad (17)$$

$$Z_i = -X_{i-1} \quad (18)$$

where $X, Y, Z = J_{x,y,z}/j$, and obey $X^2 + Y^2 + Z^2 = 1$ [9]. These equations can be obtained from Heisenberg's equations of motion in the classical limit. The fixed points at the poles $Y = \pm 1$ and the equatorial 4 period cycle $Z = 1 \rightarrow X = 1 \rightarrow Z = -1 \rightarrow X = -1$ are of special relevance to us; each of these exists for all κ_0 values. In the quantum case, these fixed points and this cycle correspond to $|\hat{\mathbf{y}}, \pm j\rangle$ and $|\hat{\mathbf{z}}, j\rangle$ respectively.

As κ_0 increases, new fixed points and cycles are born, and on further increase, they become unstable, to bifurcate into new fixed points and cycles. The game starts at $\kappa_0 = 2$, when the fixed points at $Y = \pm 1$ lose their stability, giving rise to two new FPs. By $\kappa_0 = 3$, most of the sphere becomes chaotic, but there are some significant islands of stability, notably the ones around new fixed points and one around the 4 period cycle mentioned above, which loses stability at π ; it is stable whenever $(2 \cos \kappa_0 + \kappa_0 \sin \kappa_0)^2 < 4$. At $\sqrt{2}\pi \sim 0.442$, these FPs become unstable as well. By $\kappa_0 = 6$, system is essentially fully chaotic. See [9, 10] for details.

B. Quantum Dynamics

1. Dynamics for initial state $|\hat{\mathbf{z}}, j\rangle$

We will find it convenient to move back and forth between the J_z and J_x basis. From (2) it follows that the projectors $Z_m = |\hat{\mathbf{z}}, m\rangle \langle \hat{\mathbf{z}}, m|$ and $X_m = |\hat{\mathbf{x}}, m\rangle \langle \hat{\mathbf{x}}, m|$ obey

$$TZ_mT^{-1} = Z_m; \quad R^2Z_mR^{-2} = Z_{-m}; \quad RZ_mR^{-1} = X_m; \quad RX_mR^{-1} = Z_{-m}. \quad (19)$$

Note that for $\kappa_0 = 0$, the dynamics is trivial. We have a rotating vector starting on Z_j , which goes to the J_x eigenstate X_j , followed by Z_{-j} and finally back to X_j , completing the cycle. For small but non-zero κ_0 , $T \neq 1$. Simplifying TX_jT^{-1} by using Baker-Hausdorff formula, [23]

$$TX_jT^{-1} = X_j - \frac{i\kappa_0}{2j}[J_z^2, X_j] - \frac{\kappa_0^2}{4j^2}[J_z^2, [J_z^2, X_j]] \cdots \quad (20)$$

Using $K_{\pm} = J_y \pm iJ_z$, in analogy to standard raising and lowering operators, after some calculations, one finds

$$[J_z^2, X_j] = \frac{1}{2}\sqrt{j(2j-1)}(|\hat{\mathbf{x}}, j\rangle \langle \hat{\mathbf{x}}, j-2| - |\hat{\mathbf{x}}, j-2\rangle \langle \hat{\mathbf{x}}, j|) \quad (21)$$

and $[J_z^2, [J_z^2, X_j]]$ carries terms like $X_{j-2}, X_j, |\hat{\mathbf{x}}, j-2\rangle \langle \hat{\mathbf{x}}, j|, |\hat{\mathbf{x}}, j\rangle \langle \hat{\mathbf{x}}, j-4|$.

For small κ_0 , we may neglect the higher order terms, to conclude that operation of T produces some extra off diagonal terms and mixes X_j with nearby states. Because the “ladder” is at an end for $m = j$, we only got the lower state X_{j-2} , but for $m \neq \pm j$, we do get neighbours on both sides. Note that the immediate neighbours are not mixed in the process.

After a rotation, $X_m \rightarrow Z_{-m}$. The off-diagonal J_x terms also rotate, in a sense. Note that $R^4 = \pm 1$, and the fact that R cannot distinguish between z axis and x axis. It can only do a counter-clock rotation by $\pi/2$ of each of their eigenstates, giving the same phase ϕ_m for X_\pm and Z_\pm , if any. Therefore,

$$R|\hat{\mathbf{x}}, m\rangle\langle\hat{\mathbf{x}}, n|R^{-1} = \phi_{mn}|\hat{\mathbf{z}}, m\rangle\langle\hat{\mathbf{z}}, n|. \quad (22)$$

Torsion does nothing to the Z 's, whereas the off-diagonal J_z terms again pick up opposite phases, but clearly, the magnitude of the off-diagonal is not affected. This explains how the coherence (11) increases in both J_z and J_x basis with increase in κ_0 .

As κ_0 increases, the higher order terms become relevant and as a result the mixing becomes stronger. For such cases, a single kick can mix several $\{X_m\}$ states.

2. Dynamics for $|\hat{\mathbf{y}}, j\rangle$

Defining $Y_m = |\hat{\mathbf{y}}, m\rangle\langle\hat{\mathbf{y}}, m|$, it follows from (2) that

$$RY_mR^{-1} = Y_m; \quad \bar{R}X_m\bar{R}^{-1} = Y_m; \quad TY_mT^{-1} = \bar{R}(TX_mT^{-1})\bar{R}^{-1} \quad (23)$$

where $\bar{R} = \exp(-iJ_z\pi/2)$. For $\kappa_0 = 0$, the state is invariant because it is an eigenstate of R . For $\kappa_0 > 0$, it is clear that behavior is similar to what we had before. The action of T on Y_m is just like its action on X_m 's, and mixes neighbouring states in J_y basis too. Of course, this should be expected from symmetry between x and y axes with respect to z axis.

-
- [1] A. J. Leggett and Anupam Garg. Quantum mechanics versus macroscopic realism: Is the flux there when nobody looks? *Phys. Rev. Lett.*, 54:857–860, Mar 1985.
 - [2] A J Leggett. Testing the limits of quantum mechanics: motivation, state of play, prospects. *Journal of Physics: Condensed Matter*, 14(15):R415–R451, apr 2002.
 - [3] Johannes Kofler and Časlav Brukner. Condition for macroscopic realism beyond the leggett-garg inequalities. *Phys. Rev. A*, 87:052115, May 2013.
 - [4] Clive Emary, Neill Lambert, and Franco Nori. Leggett–garg inequalities. *Reports on Progress in Physics*, 77(1):016001, dec 2013.

- [5] Lucas Clemente and Johannes Kofler. Necessary and sufficient conditions for macroscopic realism from quantum mechanics. *Phys. Rev. A*, 91:062103, Jun 2015.
- [6] Lucas Clemente and Johannes Kofler. No fine theorem for macrorealism: Limitations of the leggett-garg inequality. *Phys. Rev. Lett.*, 116:150401, Apr 2016.
- [7] J. J. Halliwell. Comparing conditions for macrorealism: Leggett-garg inequalities versus no-signaling in time. *Phys. Rev. A*, 96:012121, Jul 2017.
- [8] Florian Fröwis, Pavel Sekatski, Wolfgang Dür, Nicolas Gisin, and Nicolas Sangouard. Macroscopic quantum states: Measures, fragility, and implementations. *Rev. Mod. Phys.*, 90:025004, May 2018.
- [9] F. Haake, M. Kuś, and R. Scharf. Classical and quantum chaos for a kicked top. *Zeitschrift für Physik B Condensed Matter*, 65(3):381–395, Sep 1987.
- [10] F. Haake. *Quantum Signatures of Chaos*. Springer-Verlag, Berlin, 1991.
- [11] Asher Peres. *Quantum Theory: Concepts and Methods*. Kluwer Academic Publishers, New York, 2002.
- [12] Shohini Ghose and Barry C. Sanders. Entanglement dynamics in chaotic systems. *Phys. Rev. A*, 70:062315, 2004.
- [13] S. Chaudhury, A. Smith, B. E. Anderson, S. Ghose, and P. S. Jessen. Quantum signatures of chaos in a kicked top. *Nature*, 461:768, 2009.
- [14] C. Neill, P. Roushan, M. Fang, Y. Chen, M. Kolodrubetz, Z. Chen, A. Megrant, R. Barends, B. Campbell, B. Chiaro, A. Dunsworth, E. Jeffrey, J. Kelly, J. Mutus, P. J. J. O’Malley, C. Quintana, D. Sank, A. Vainsencher, J. Wenner, T. C. White, A. Polkovnikov, and J. M. Martinis. Ergodic dynamics and thermalization in an isolated quantum system. *Nature Physics*, 12:1037, 2016.
- [15] Shruti Dogra, Vaibhav Madhok, and Arul Lakshminarayan. Quantum signatures of chaos, thermalization, and tunneling in the exactly solvable few-body kicked top. *Phys. Rev. E*, 99:062217, Jun 2019.
- [16] A. W. van der Vaart. *Asymptotic Statistics*. Cambridge Series in Statistical and Probabilistic Mathematics. Cambridge University Press, 1998.
- [17] T. Baumgratz, M. Cramer, and M. B. Plenio. Quantifying coherence. *Phys. Rev. Lett.*, 113:140401, Sep 2014.

- [18] For a uniform random variable t_β , such a time average correctly gives the ensemble average for d_n . Same holds for higher moments.
- [19] Roy J. Glauber and Fritz Haake. Superradiant pulses and directed angular momentum states. *Phys. Rev. A*, 13:357, Oct 1976.
- [20] J M Radcliffe. Some properties of coherent spin states. *Journal of Physics A: General Physics*, 4(3):313–323, may 1971.
- [21] Jayendra N. Bandyopadhyay and Arul Lakshminarayan. Entanglement production in coupled chaotic systems : Case of the kicked tops. *Phys. Rev. E*, 69:016201, 2004.
- [22] Arnd Bäcker. Numerical aspects of eigenvalue and eigenfunction computations for chaotic quantum systems, 2002.
- [23] J. J. Sakurai and Jim Napolitano. *Modern Quantum Mechanics*. Cambridge University Press, 2 edition, 2017.